Dual-energy imaging performance of a sandwich detector for mouse imaging

Dong Woon Kim [a], Junwoo Kim [a], Jiwoong Park [a], Ho Kyung Kim [a,b*]
[a] *School of Mechanical Engineering, Pusan National University, Busan, Republic of Korea*
[b] *Center for Advanced Medical Engineering Research, Pusan National University, Busan, Republic of Korea*
[*] *Corresponding author: hokyung@pusan.ac.kr*

1. Introduction

In previous studies [1, 2], single-shot dual-energy imaging (DEI) was developed using a flat-panel sandwich detector. The sandwich detector consist of two scintillator-based flat-panel detectors (FPDs) between which an intermediate copper (Cu) filter layer is placed. Unlike the conventional kVp-switching dual-shot method, where motion artifacts can occur at two exposures, the single-shot DEI has the advantage of acquiring images without motion artifacts.

For the practical use of a sandwich detector for the single-shot DEI, we have developed cascaded linear-systems analysis (CSA) model [3]. We calculated the spatial-frequency-dependent performance using the CSA such as noise-power spectrum (NPS) and detective quantum efficiency (DQE). Also, we converted the spatial-frequency-dependent NPS derived from the CSA into a single-valued noise term.

In this study, we develop the contrast model and DE noise model using the CSA as a function of intermediate Cu filter thickness. And we validate the contrast model and DE noise model with experimental measurements. This models can be used to find optimal intermediate Cu filter thickness and be expanded to find various design/operation parameters for sandwich detectors.

2. Theoretical background

2.1 Performance in dual-energy images

Figure 1 is a sketch describing the virtual numerical mouse phantom and a schematic showing x-ray projections through various regions of mouse. Each region of interest (ROI) 1, 2, 3, and 4 refers to the signal depending on the material through which x-ray is transmitted. Material *j*-enhanced DE image in sandwich detectors can be obtained by the log-subtraction DE imaging algorithm such that

$$p_{jm}^{DE} = \left| w_{\hat{j}} p_m^F - p_m^R \right| = \ln\left| \left(\frac{I_m^F}{I_0^F} \right)^{w_j} - \left(\frac{I_m^R}{I_0^R} \right) \right|, \quad (1)$$

where I is a projection image and p is its log transformation. The superscripts F and R denote the front and rear images, respectively, and the subscript 0 denotes the image obtained without any object. $w_{\hat{j}}$ is the cancellation parameter to suppress the complement of material j in the DE image. Then, the contrast of j-material can be represented as a projection signal difference:

$$\begin{aligned} C_j &= \left| p_{jm}^{DE} - p_{jn}^{DE} \right| \\ &= \left| \left(w_{\hat{j}} \Delta\mu_{\mathrm{jM}}^F - \Delta\mu_{\mathrm{jM}}^R \right) t_j + \left(w_{\hat{j}} \Delta\mu_{\mathrm{jM}}^F - \Delta\mu_{\mathrm{jM}}^R \right) t_{\hat{j}} \right| \end{aligned}, \quad (2)$$

where $\Delta\mu_{\mathrm{jM}} = \mu_j - \mu_{\mathrm{M}}$, t_j and $t_{\hat{j}}$ are the thicknesses of enhanced material and subtracted material, respectively.

Using the error propagation rule, the noise of the DE image is calculated as follows [4]:

$$\sigma_j^2 = w_{\hat{j}}^2 \left(\frac{\sigma^F}{\bar{d}^F} \right)^2 + \left(\frac{\sigma^R}{\bar{d}^R} \right)^2 = \frac{w_{\hat{j}}^2}{\left(\mathrm{SNR}^F \right)^2} + \frac{1}{\left(\mathrm{SNR}^R \right)^2}. \quad (3)$$

where $\bar{d}$ and σ represent the image signal and noise, respectively. Also Eq. (3) represents that noise in DE images from a combination of SNR performances of front and rear image.

2.2 Zero-frequency DQE

The DQE is a representative detector performance and is composed of modulation transfer function (MTF) and NPS. Also, DQE can be expressed as $\mathrm{DQE}(u,v) = \mathrm{MTF}^2(u,v) / \left[\bar{q}\,\mathrm{NPS}(u,v) / \bar{d}^2 \right]$, where u and v denote the Fourier conjugates of spatial variables x and y, respectively. The zero-frequency DQE can be obtained by DQE equation at $(u,v) = (0,0)$ and which implies such that [5]

$$\mathrm{DQE}(0) = \frac{1}{\bar{q}\left[\mathrm{NPS}(0) / \bar{d}^2 \right]}, \quad (4)$$

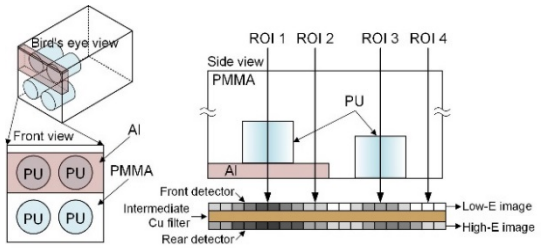

Fig. 1. Sketch describing the virtual numerical mouse phantom and schematic showing x-ray projections through various regions of a mouse consisting of bone (Al) and soft tissue (PU).

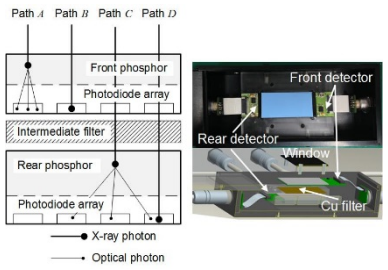

Fig. 2. The experimental setup for DE imaging and design of sandwich detectors.

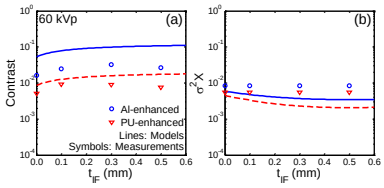

Fig. 3. Dual-energy contrast and noise performance obtained from the theoretical model and the experimental measurements as a function of intermediate Cu filter thickness. (a) DE contrast performance, and (b) DE noise performance.

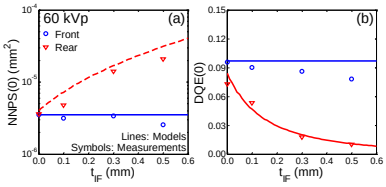

Fig. 4. Dual-energy zero-frequency performance obtained from the theoretical model and the experimental measurements as a function of intermediate Cu filter thickness. (a) zero-frequency NNPS, and (b) zero-frequency DQE.

where $\bar{q}$ denotes the incident photon fluence. The NPS at the zero-spatial frequency can be approximated to

$$\mathrm{NPS}(0) = \left[\int_{-\infty}^{\infty}\int_{-\infty}^{\infty} \mathrm{MTF}_{\mathrm{pre}}^2(u,v)\,du\,dv\right]^{-1}\sigma_d^2, \quad (5)$$
$$= A_{\mathrm{eff}}\sigma_d^2$$

where $\mathrm{MTF}_{\mathrm{pre}}$ is the presampling MTF, and A_{eff} is the effective aperture size of a detector.

Noise in *j*-material enhanced DE images can be expressed in terms of a detector performance and the photon fluence used for imaging as well as the cancellation parameter used for reconstruction:

$$\sigma_j^2 = \frac{w_j^2}{\mathrm{DQE}^F(0)\bar{q}^F A_{\mathrm{eff}}^F} + \frac{1}{\mathrm{DQE}^R(0)\bar{q}^R A_{\mathrm{eff}}^R}. \quad (6)$$

3. Materials & Methods

The sandwich detectors are fabricated by stacking two detectors as shown in Fig. 2, each of which employs a combination of a Gd_2O_2S:Tb phosphor screen (Carestream Health Inc., Rochester, NY) and a photodiode array (RadEye1™, Teledyne Rad-icon Imaging Corp., Sunnyvale, US) having 512×1024 pixels with a pixel pitch (*p*) of 0.048 mm. Thickness of phosphor layers is ~34 mg cm^{-2} and ~ 67 mg cm^{-2} for the front and rear detectors, respectively.

We evaluate the performance of DE images using a figure of merit (FOM). We may define the FOM in DE images using the contrast-to-noise ratio (CNR) as a "benefit" and the total exposure invested for imaging as a "cost" such that

$$\mathrm{FOM}_j = \frac{\mathrm{CNR}_j^2}{X^{\mathrm{tot}}}, \quad (7)$$
$$= C_j^2\left[X^{\mathrm{tot}}\left(\frac{w_j^2}{\mathrm{DQE}^F(0)\bar{q}^F A_{\mathrm{eff}}^F} + \frac{1}{\mathrm{DQE}^R(0)\bar{q}^R A_{\mathrm{eff}}^R}\right)\right]^{-1}$$

where C_j refers to the contrast in a *j*-enhanced DE image and X^{tot} denotes the total exposure.

4. Preliminary results

The theoretical model describes reasonably the measured DE contrast and noise performance as shown in Fig. 3. The measured DE contrast performance is slightly decreased at increasing thickness of intermediate Cu filter. However, the DE contrast performance of theoretical model is increased at increasing thickness of intermediate Cu filter. The noise performance is slightly decreased at increasing thickness of intermediate Cu filter as shown in Fig. 3(b). As the intermediate Cu filter thickness increases in the experiment, the quality of the image deteriorates because the number of photons obtained from the rear detector decreases.

The zero-frequency performance of the front detector is nearly independent intermediate Cu filter shown in Fig. 4(a) and (b). But zero-frequency NNPS of the rear detector is increased as shown in Fig. 4(a), and the zero-frequency DQE of rear detector is exponentially decreased as shown in Fig. 4(b). The theoretical zero-frequency performance can describe the measured performance well.

5. Ongoing and Further Studies

Further analysis of the FOM of DE images is under progress. In addition, we are going to analyze the optimal intermediate Cu filter thickness using FOM model for the single-shot DEI. This study will be very useful for designing and optimizing sandwich detectors for single-shot DEI.

ACKNOWLEDGEMENT

This work was supported by the National Research Foundation of Korea (NRF) grants funded by the Korea governments (MSIP) (No. 2014R1A2A2A01004416).

REFERENCES

[1] S. Yun, J. C. Han, D. W. Kim, H. Youn, H. K. Kim, J. Tanguay, and I. A. Cunningham, Feasibility of active sandwich detectors for single-shot dual-energy imaging, Proc. SPIE 9033, pp. 90335T-90335T-8, 2014.
[2] J. C. Han, H. K. Kim, D. W. Kim, S. Yun, H. Youn, S. Kam, J. Tanguay, and I. A. Cunningham, Single-shot dual-energy x-ray imaging with a flat-panel sandwich detector for preclinical imaging, Cur. Appl. Phys., Vol. 14, No. 12, pp. 1734-1743, 2014.
[3] D. W. Kim, J. Kim, S. Yun, H. Youn, and H. K. Kim, Cascaded-systems analysis of sandwich x-ray detectors, J. Instrum., Vol. 11, No. 12, p. C12022, 2016.
[4] S. Richard, J. H. Siewerdsen, D. A. Jaffray, D. J. Moseley, and B. Bakhtiar, Generalized DQE analysis of radiographic and dual-energy imaging using flat-panel detectors, Med. Phys., Vol. 32, No. 5, pp. 1397-1413, 2005.
[5] I. A. Cunningham, Handbook of Medical Imaging, Vol. 1. Physics and Phsychophysics, ch. 2, pp. 79-160. Edited by J. Beutel, H. L. Kundel, R. L. Van Metter (SPIE, Bellingham, WA), 2000.